Synthesis, characterization, molecular modeling, and DNA interaction studies of a Cu(II) complex containing drug of chronic hepatitis B: adefovir dipivoxil

Nahid Shahabadi, Monireh Falsafi & Soraya Moradi Fili

Taylor & Francis
Taylor & Francis Group

Synthesis, characterization, molecular modeling, and DNA interaction studies of a Cu(II) complex containing drug of chronic hepatitis B: adefovir dipivoxil

NAHID SHAHABADI*, MONIREH FALSAFI and SORAYA MORADI FILI

Faculty of Science, Department of Chemistry, Razi University, Kermanshah, Iran
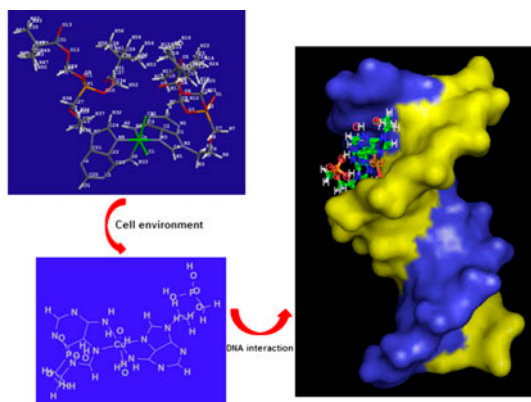
A new copper(II) complex [Cu(adefovir)$_2$Cl$_2$], where adefovir = adefovir dipivoxil drug, was synthesized and characterized by using different physicochemical methods. Binding interaction of this complex with calf thymus DNA (ct-DNA) has been investigated by multi-spectroscopic techniques and molecular modeling study. The complex displays significant binding properties of ct-DNA. The results of fluorescence and UV–vis absorption spectroscopy indicated that, this complex interacted with ct-DNA in a groove-binding mode, and the binding constant was $4.3(\pm0.2) \times 10^4$ M^{-1}. The fluorimeteric studies showed that the reaction between the complex and ct-DNA is exothermic (ΔH = 73.91 kJ M$^{-1}$; ΔS = 357.83 J M^{-1} K^{-1}). Furthermore, the complex induces detectable changes in the CD spectrum of ct-DNA and slightly increases its viscosity which verified the groove-binding mode. The molecular modeling results illustrated that the complex strongly binds to the groove of DNA by relative binding energy of the docked structure −5.74 kcal M^{-1}. All experimental and molecular modeling results showed that the Cu(II) complex binds to DNA by a groove-binding mode.

Keywords: Copper(II) complex; Groove binder; Adefovir dipivoxil; DNA interaction

*Corresponding author. Email: n.shahabadi@razi.ac.ir

1. Introduction

Adefovir dipivoxil is a diester prodrug of the antiviral drug adefovir, with much larger oral bioavailability than adefovir. Evidence demonstrates that the prodrug is metabolized to adefovir in the enterocytes during intestinal absorption [1]. Adefovir, an acyclic nucleoside phosphonate, is a reverse transcriptase inhibitor with antiviral activity against a wide range of viruses such as retroviruses, immuno-deficiency virus types 1 and 2 (HIV1 and HIV2), and herpes viruses [1, 2]. Adefovir acts by blocking reverse transcriptase enzyme, an enzyme that is crucial for the hepatitis B virus (HBV) to reproduce in the body [3].

Metal complexes have been widely applied in medicine for centuries, although their molecular mechanism has not yet been fully understood [4, 5]. Metal ions present in complexes not only accelerate drug action by forming coordination complexes with them, but also enhance the effectiveness of the organic ligands [6, 7]. The medicinal properties of metal complexes depend on the nature of the metal ions and the ligands [8, 9]. Interest in preparation of new metal complexes has forced the study of the interaction of metal complexes with DNA for their potential applications in medicine [10]. DNA is a primary intracellular target of antitumor drugs, and interactions of DNA with transition metal complexes range from intercalation to covalent and groove binding [11, 12]. Thus, research on the mechanism of the interaction of complexes with DNA is important for the design of efficacious drug entities, which exhibit different properties than the mainstream protocol drugs viz. cisplatin, etc., which are currently in use [13, 14].

Copper with its bioessential activity and oxidative nature has attracted attention to address Cu(II) complexes for the medical applications [15–20]. Copper(II) complexes containing heterocyclic bases have been explored in virtue of their strong interactions with DNA and cytotoxic activity [19]. Many copper complexes were synthesized and their interaction with DNA was investigated. Different modes of interactions were reported, such as intercalation [21–26] or groove binding [27]. These complexes can be used for the development of anticancer drugs.

The development of anticancer drugs is slow and costly. One approach to accelerate the availability of new drugs is to reposition drugs like adefovir dipivoxil, which are approved for other indications as anticancer agents. In our laboratory, we have focused our attention to design improved drugs that target cellular DNA to understand the mechanism of action at the molecular level, and also to investigate the effect of drugs as anticancer agents. Therefore, information obtained from this study will be helpful in understanding the mechanism of interaction of this complex with nucleic acids, and will be useful in the development of potential probes of DNA structure and conformation and new therapeutic reagents for cancer.

We have recently reported the binding affinity of adefovir dipivoxil with ct-DNA using multiple spectroscopic techniques and molecular modeling [28]. The results indicated that the drug interacted with ct-DNA in a groove-binding mode with the binding constant $3.3(\pm0.2) \times 10^4\,M^{-1}$ [29]. Within this study, we focus on the synthesis of a copper complex of adefovir dipivoxil to improve the antiviral drug as an anticancer agent. Binding studies of this complex with ct-DNA were investigated using multiple spectroscopic techniques, such as absorption spectroscopy, emission spectroscopy, and circular dichroism. Dynamic viscosity measurements were used. Molecular modeling results were applied for verifying the results of spectroscopic methods and for illustrating the binding mode.

2. Materials and methods

2.1. *Materials*

Commercially pure chemicals, Tris–HCl (Sigma Co., Madrid, Spain), highly polymerized calf thymus-DNA (ct-DNA) (Sigma Co., Madrid, Spain), and copper chloride (Sigma Co.) were procured and used without purification. Adefovir dipivoxil (9-[2-[bis[(pivaloyloxy) methoxy]-phosphinyl]methoxy]ethyl]adenine) was purchased from OSR Health care Pvt Ltd. company of India. All experiments were carried out in Tris–HCl buffer solutions prepared in double-distilled water (10 mM, pH 7.4). Stock solution of ct-DNA was prepared by dissolving 2 mg of ct-DNA fibers in 2 mL Tris–HCl (pH 7.4) buffer and storing it for 24 h at 4 °C. The concentration of DNA in stock solution (1×10^{-3} M) was expressed in monomer units, as distinguished by spectrophotometry at 260 nm using an extinction coefficient (ε_p) of 6600 M^{-1} cm^{-1}, while DNA solutions were applied after no more than four days.

2.2. *Synthesis of copper(II) complex*

The specific procedure to prepare the adefovir dipivoxil–copper complex is as follows: 0.204 g (2 mM) of drug was added to 30 mL of boiling ethanol. Similarly, 0.034 g (1 mM) of copper chloride was added in 5 mL ethanol. The two above-prepared solutions were mixed and the mixture was refluxed for 1 h. The obtained green solution was dried and the resultant green powder was collected, washed with H_2O, and dried in air (47% yield). The complex (figure 1) is soluble in ethanol, DMF, and DMSO. Based on elemental analysis data, the possible structure was [Cu(adefovir)$_2$(Cl)$_2$]. Anal. Found (%) for $C_{40}H_{64}N_{10}O_{16}P_2$-$CuCl_2$: C, 42.81; H, 5.83; N, 12.21. Calcd (%): C, 42.24; H, 5.67; N, 12.31.

2.3. *Instrumentation*

To characterize and assess the structure of the complex, C, H, and N data were obtained by using a Costech ECS 4010 elemental analyzer. FT-IR spectra were recorded on a Perkin–Elmer spectrometer in KBr pellets from 400 to 4000 cm^{-1}. FAR-IR spectra were
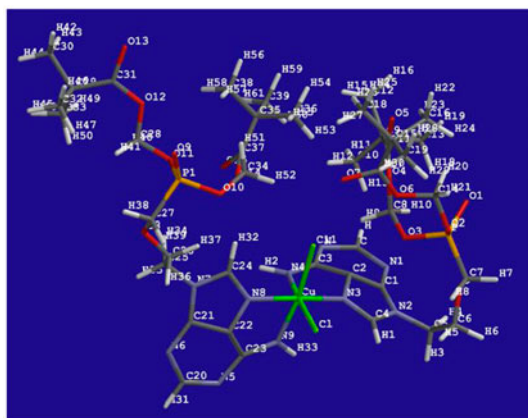

Figure 1. The chemical structure of [Cu(adefovir)$_2$Cl$_2$].

recorded on a Bruker Vertex 70 spectrometer in CsI pellets from 30 to 600 cm^{-1}. The ^{1}H-NMR spectra were obtained on a Bruker Avance 300 MHz spectrometer operating at room temperature. Raman spectra were recorded on a Bruker FRA106/S spectrometer from 80 to 4000 cm^{-1}. XRD was recorded on an Inel EQUINX3000 instrument.

Absorbance spectra were recorded using an HP spectrophotometer (Agilent 8453) equipped with a thermostated bath (Huber polysat cc1). Absorbance measurements were performed by keeping the complex concentration constant (2.5×10^{-5} M), while varying the ct-DNA concentration from 0 to 8.0×10^{-5} M (r_i = [DNA]/[complex] = 0.0–3.2). The spectra were recorded from 200 to 500 nm.

CD measurements were recorded on a JASCO (J-810) spectropolarimeter, keeping the concentration of DNA constant (5×10^{-5} M), while varying the complex concentration from 0 to 3.0×10^{-5} M (r_i = [complex]/[DNA] = 0.0–0.6).

Viscosity measurements were made using a viscometer (SCHOT AVS 450) at 25 °C $\pm$ 0.5 °C in a constant temperature bath, while the DNA concentration was fixed at 5×10^{-5} M and flow time was measured with a digital stopwatch. The data are reported as $(\eta/\eta_0)^{1/3}$ *versus* $1/r$ (r =[complex]/[DNA] = 0.0–1.0), where η_0 is the viscosity of the DNA solution alone.

All fluorescence measurements were performed on a JASCO spectrofluorimeter (FP6200) using a quartz cell of 1 cm path length by keeping the concentration of the complex constant (1×10^{-5} M^{-1}), while varying the DNA concentration from 0 to 3.4×10^{-5} M at three different temperatures (293, 310, and 318 K). Samples were excited at 260 nm and emission spectra were recorded from 300 to 480 nm.

Quenching experiments were conducted by adding small stoichiometric aliquots of potassium iodide stock solution (0.1 M) to the copper complex and ct-DNA–copper complex solutions, respectively. The fluorescence intensity was recorded and the quenching constants (K_{sv}) were calculated.

2.4. *Molecular docking study*

MGL tools 1.5.4 with AutoGrid4 and AutoDock4 were used to set up and perform blind docking calculations between the copper complex and DNA sequence [30]. DNA sequence d(CGCGAATTCGCG)$_2$ dodecamer (PDB ID: 1BNA) was obtained from the Protein Data Bank. Receptor (DNA) and ligand (the complex) files were prepared using AutoDock Tools. The DNA (1BNA) was enclosed in a box with number of grid points in $x \times y \times z$ directions, $64 \times 74 \times 124$, and a grid spacing of 0.375 Å. The center of the grid was set to 14.78, 20.976, and 8.807 Å. Lamarckian genetic algorithms, as implemented in Auto-Dock, were applied to perform docking calculations. The structures of molecules were drawn and optimized using Spartan '10 package. All the molecular images and animations were shaped using PyMol [31].

3. Results and discussion

3.1. *Synthesis and characterization of the copper(II) complex*

[CuCl$_2$(adefovir)$_2$] was prepared from CuCl$_2$ with two equivalents of purified drug in ethanol at room temperature (figure 1). In the IR spectra, the N–H stretches (NH$_2$) of free drug were observed at 3365 and 3275 cm^{-1}, whereas in the drug–copper complex the N–H

stretching (NH$_2$) vibrations were observed at 3442 and 3353 cm^{-1}, respectively. The N–H bending in free drug is at 1605 cm^{-1}, while after complexation shifted to 1609 cm^{-1}. This indicates the metal–nitrogen bond (figure S1, see online supplemental material at http://dx.doi.org/10.1080/00958972.2015.1013945).

New band at 524 cm^{-1} in the spectrum of the complex corresponds to νM-N (figure S1). The appearance of νM-N supports the involvement of NH$_2$ in complexation with metal ion [32]. Also two new bands at 279 and 342 cm^{-1} were observed in FAR-IR spectrum for the complex that corresponds to Cu–Cl and Cu–N bands (figure S2). The Cu–N band in the FAR-IR spectrum corresponds to N in the five-membered ring [33, 34]. Bands were observed at 230 cm^{-1} and 209 cm^{-1} in the Raman spectrum of the drug-copper complex (figure S3). These two bands were assigned as N–Cu–N bending (N in five-membered ring) and Cu–Cl stretching modes, respectively.

The ^{1}H-NMR spectrum of the complex validates Cu(II) coordination to the drug ligand. Conductivity measurements were performed in DMF (molar conductance, Λ_M (1×10^{-3} M in DMF 25.47 Ω^{-1} cm^2 M^{-1}) and confirmed the non-electrolytic nature of the complex [35]. The nature of the complex was also ascertained by powder X-ray diffraction studies. The XRD pattern indicates the microcrystalline nature of the complex as shown in figure S4. Diffraction peaks were observed at scattering angles (2θ) of 13.01, 18.5, 21.02, 25.8, 31.1, 35.88, and 44.02 which correspond to reflections from 002, 111, 202, 004, 114, 313, and 224 crystal planes, respectively, which is the characteristic feature of the orthorhombic crystal system of the complex. The lattice parameters calculated from XRD are $a = 10.406$ Å, $b = 5.94$ Å, and $c = 13.697$ Å with cell volume 846.63 Å^3, which revealed the structure is same as that of bulk (JCPDF No. 00-045-0025, [Cu(NO$_2$)$_2$(NH$_3$)$_4$]). These parameters further indicate the cubic crystal structure with space group Ccc2 (37).

3.2. DNA binding studies

3.2.1. Electronic absorption spectra. The binding mode of the complex with ct-DNA was investigated using electronic absorption spectra [36]. Binding of a complex with DNA via intercalation generally results in hypochromism and a red-shift of the absorption band (bathochromic effect) because of strong interaction between the ligand and the base pairs of the DNA [37, 38]. In groove binding between DNA and small molecules, hyperchromism can be observed, while the position of the absorption almost does not change, which can be associated with degradation of the DNA double-helix structure [39, 40]. Electronic spectra of the complex in the absence and presence of ct-DNA are given in figure 2. In the presence of increasing concentration of ct-DNA, the complex exhibited hyperchromism with almost no shift at 260 nm. These results suggest that the interaction of the complex with ct-DNA is non-intercalative and can be rationalized in terms of groove binding. The changes in absorbance with increasing amounts of ct-DNA were used to evaluate the intrinsic binding constant, K_b, for the copper complex. The intrinsic binding constant, K_b, was calculated by using equation (1) and monitoring the changes in the 260 nm band with increasing concentration of ct-DNA:

$$\frac{[\text{DNA}]}{(\varepsilon_a - \varepsilon_f)} = \frac{[\text{DNA}]}{(\varepsilon_b - \varepsilon_f)} + \frac{1}{K_b(\varepsilon_b - \varepsilon_f)} \tag{1}$$

where [DNA] is the concentration of DNA, ε_a, ε_f, and ε_b corresponds to the apparent extinction coefficient, the extinction coefficient for the free compound, and its entirely
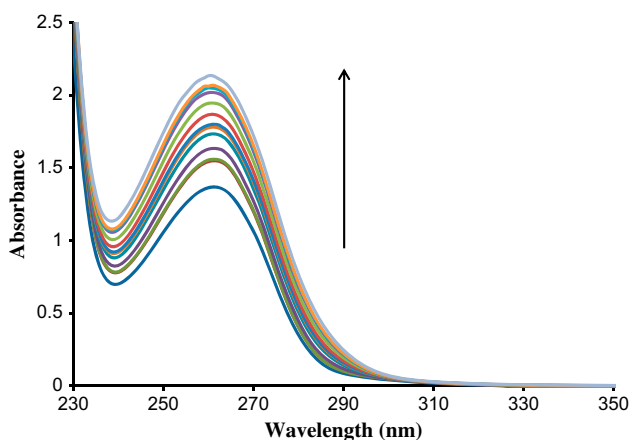
Figure 2. Absorption spectra of copper(II) complex $(2.5 \times 10^{-5}$ M) in the absence and presence of increasing amounts of ct-DNA: r_i = 0.0, 0.13, 0.25, 0.44, 0.75, 1.06, 1.37, 1.68, 1.99, 2.30, 2.6, 2.9, and 3.2.

DNA-bound combination, respectively. K_b was given by the plots of $[DNA]/(\varepsilon_a - \varepsilon_f)$ *versus* [DNA] from the ratio of the slope to intercept (figure S5). The binding constant, K_b, for the complex was $4.3(\pm0.2) \times 10^4$ M^{-1}. This K_b value is slightly larger than adefovir dipivoxil $(3.3(\pm0.2) \times 10^4$ M$^{-1})$ and is similar to those reported for well-established groove-binding agents, such as sesamol $(2.7 \times 10^4$ M$^{-1})$ [41], salmeterolxinafoate $(8.52 \times 10^3$ M$^{-1})$ [42], $[Cr(salprn)(H_2O)_2]^+$ $(1.7(\pm0.3) \times 10^4$ M$^{-1})$ [43], isoxazolcurcumin $(10^4$ M$^{-1})$ [44], amsacrine $(1.2(\pm0.1) \times 10^4$ M$^{-1})$ [45], $[Cu_2(L\text{-}trp)L(H_2O)](NO_3)_2$ $(2.4 \times 10^4$ M$^{-1})$ [46], mono metallic complex containing 1,10-phenanthroline and indole-3-acetic acid$(C_{32}H_{24}N_4O_4Co)$ $(1.02 \times 10^4$ M$^{-1})$ [47], Cu(II) complexes of Schiff base ligands $(1.4 \times 10^4$ and 4.5×10^4 M$^{-1})$ [47, 48], $[Cu(HL)_2]\cdot1.5ClO_4\cdot0.5OH$ (where HL = (E)-N'-(1-(pyridine-2yl)ethylidene) benzohydrazide $(4.66 \times 10^4$ M$^{-1})$ [49], and $[Cu_2(\mu\text{-}Cl)_2(O\text{-}2\text{-alkoxyethylpyridine-2-}$ carboximidate)$_2Cl_2]$ $(6.36 \times 10^2$ M$^{-1})$ [50].

Binding mode between the Cu(II) complex containing adefovir dipivoxil and DNA was groove binding.

3.2.2. Viscosity measurements. Hydrodynamic methods that are sensitive to length are regarded as one of the most critical tests of a binding mode in solution, where crystallographic structural data are not available. Intercalating agents are expected to elongate the double helix because of incorporating the compound in between the base leads to an increase in the viscosity of DNA [51]. In contrast, the complexes bind exclusively in the DNA grooves by partial and/or non-classical intercalation, under the same conditions, typically cause less (positive or negative) or no change in DNA solution viscosity [52]. The values of $(\eta/\eta_0)^{1/3}$ were plotted against [DNA]/[Cu complex], where η and η_0 are the relative viscosities of DNA in the presence and absence of the complex, respectively (figure 3). The plot of figure 3 reveals that the drug shows little change in DNA viscosity, which is consistent with DNA groove binding [53].

3.2.3. CD spectral studies. Circular dichroism (CD) spectroscopy gives valuable information on how the conformation of DNA is influenced by the binding of the metal complex to
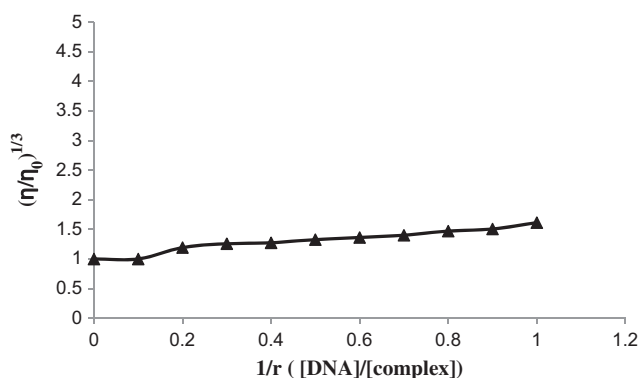
Figure 3. Effect of increasing concentration of complex on the relative viscosity of ct-DNA at 25 °C.

DNA. The observed CD spectrum of calf thymus DNA consists of a positive band at 275 nm due to base stacking, and also a negative band at 248 nm due to helicity, which is characteristic of DNA in the right-handed B form. While groove binding and electrostatic interaction of small molecules with DNA show little or no perturbations on the base-stacking and helicity bands, classical intercalative ligands tend to enhance the intensities of bands due to strong base-stacking interactions and stable DNA conformations [40]. The CD spectra of DNA in the presence of the complex are illustrated in figure 4 and exhibit a decrease in both the positive and negative bands. Decrease in molar ellipticity at these bands (275 and 248 nm) suggests distortion in native conformation of B-DNA due to interaction with the complex. These spectral variations show the presence of some ct-DNA features in native conformation of DNA upon interaction. Moreover, reduction in 248 nm CD band is considered as a key marker of C-form of DNA [54, 55]. However, it seems that the perturbation in DNA conformation is limited to few base pairs because, when complete B to C transition occurs, then the CD band at 248 nm shows about 66% decrease in its intensity. However, not much decrease in the concerned band is observed. Consequently, there are possibilities of the formation of an intermediate form of DNA having features of
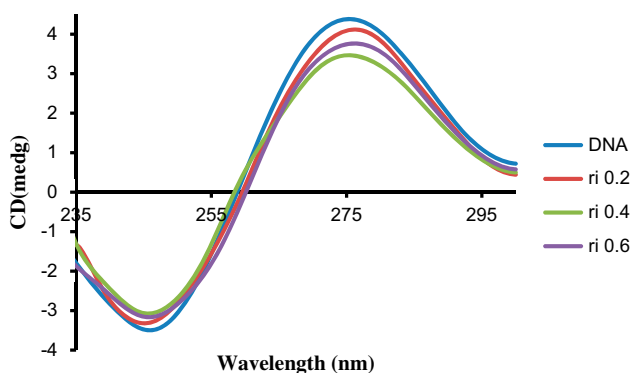

Figure 4. CD spectra of DNA (5×10^{-5} M) in 10 mM Tris–HCl buffer in the presence of increasing amounts of Cu(II) complex (r_i = [complex]/[DNA] = 0.0, 0.2, 0.4, 0.6).

both B and C conformation. Similar results have been observed in the case of cationic lipid and neutral lipid binding with DNA that have been ascribed to a non-cooperative augment in DNA [56, 57]. Increase in winding angle (or decrease in propeller twist) causes widening in the DNA groove that enables proper positioning of small molecules in the groove pocket [58].

3.2.4. Fluorescence studies. Fixed amounts (1×10^{-5} M) of the copper complex were titrated with increasing amounts of ct-DNA. The complex emits luminescence in Tris–HCl buffer with a maximum at 347 nm upon excitation at 260 nm. The fluorescence titration spectra of the complex in the absence and presence of ct-DNA at 10 °C are given in figure 5. As shown in this figure, the fluorescence intensity of the complex is quenched steadily with increasing concentration of ct-DNA. This may be ascribed to photoelectron transfer from the guanine base of DNA to the excited levels of the complex [59, 60].

Quenching is carried out by different mechanisms, classified as dynamic and static quenching. Dynamic quenching refers to a process in which the fluorophore (here the complex) and the quencher (DNA) comes into contact during the transient existence of the excited state, but static quenching refers to fluorophore–quencher complex formation. In general, dynamic and static quenching has differing dependence on temperature and excited state lifetime. The dynamic quenching process increases with increase in temperature because upon this condition the compounds move faster, which cause more collision probability. The formation of composite is responsible for the static quenching; hence, increase in the temperature diminishes the stability of the composite and causes decrease in fluorescence quenching [61]. Since, in both cases, the fluorescence intensity is related to the
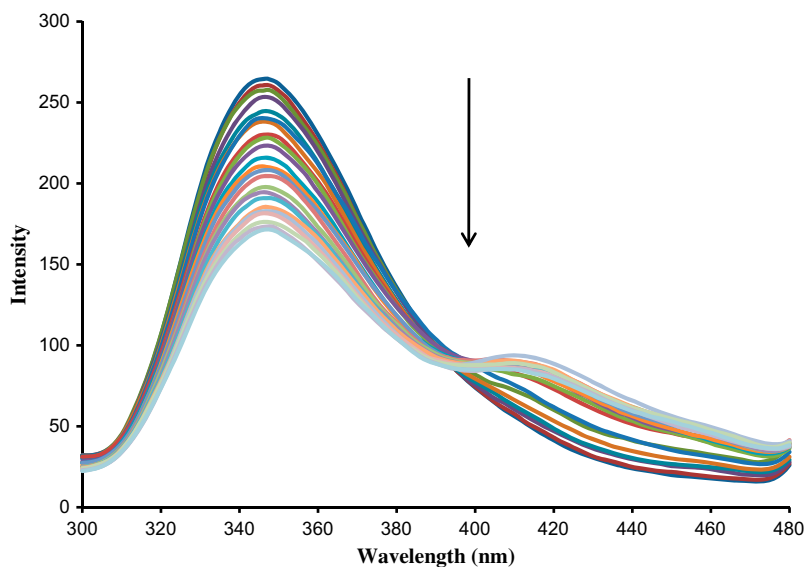

Figure 5. The fluorescent spectral characteristics of the complex–DNA at 283°K. The complex concentration: 1×10^{-5} M at pH 7.4. DNA concentrations: 0.0, 0.158, 0.32, 0.47, 0.63, 0.79, 0.945, 1.10, 1.57, 1.73, 1.88, 2.04, 2.2, 2.35, 2.51, 2.66, 2.81, 2.97, 3.13, 3.28, and 3.44 × 10^{-5} M.

concentration of the quencher (DNA), the quenched fluorophore can be used as an indicator for the quenching agent [62].

Fluorescence quenching is described by the Stern–Volmer equation [equation (2)]:

$$F_0/F = 1 + K_{sv}[Q] \qquad (2)$$

where F_0 and F represent the fluorescence intensities in the absence and in the presence of ct-DNA, respectively, K_{sv} is the quenching constant, and $[Q]$ is the concentration of the quencher [63]. In our experiments, with the temperature increasing from 10 °C to 37 °C, the Stern–Volmer constant (K_{sv}) increased from $1.7(\pm0.02) \times 10^4 \, M^{-1}$ to $2.5 (\pm0.02) \times 10^4 \, M^{-1}$ for the complex (figure S6) indicating that the mechanism of the quenching may be dynamic quenching, but static quenching cannot be excluded. These two kinds of quenching mechanisms demonstrate some differences that can be distinguished experimentally, such as change in the absorption spectrum of DNA and temperature dependence of the quenching constant [64]. In static quenching, a complex between DNA and copper complex forms, so there will be some changes in the UV–visible spectrum of DNA, whereas, dynamic quenching has no such change. Diffusion is the control step for dynamic quenching, so the quenching constant will enhance with increase in the temperature [65]. Most fluorescence quenching is in accord with this theory and fits the results [66]. Thus, we employed electronic absorption spectra to give evidence for the actual quenching process. The UV–visible absorption spectra of the complex and the DNA-complex system were measured. According to the theory, the UV spectrum of the complex would have no detectable changes, if the quenching was a dynamic mechanism [67], but ground-state DNA–copper compound is formed in the static quenching, and the UV spectrum of the copper complex changes [68]. Therefore, according to the UV spectra, the fluorescence quenching of the complex in our case seems to be primarily caused by complex formation between the copper compound and DNA. Therefore, it is suggested that the effect of quencher may be due to a combination of static and dynamic quenching.

The binding constant (K_f) and the binding stoichiometry (n) for the complex formation between the complex and DNA were assayed using equation (3) [63]:

$$\log (F_0 - F/F) = \log K_f + n \log [Q] \qquad (3)$$

where F_0 and F are the fluorescence intensities of the complex in the absence and presence of different concentrations of ct-DNA, respectively, and n is the number of equivalent binding sites, which can be revealed by the slope based on equation (3).

In the present study, the binding constants of the complex were obtained at various temperatures (table 1). Since $n = 1$, a 1 : 1 adduct is formed (figure S7). The value of K_f for the copper complex at room temperature is comparable to the hetero-bimetallic complex containing 1,10-phenanthroline and indole-3-acetic ($C_{32}H_{30}O_8N_4CuSn_2Cl_6$) ($4.09 \times 10^4 \, M^{-1}$) [46],

Table 1. Binding constants (K_f), number of binding sites (n), and relative thermodynamic parameters for the binding of $[Cu(adefovir)_2Cl_2]$ to ct-DNA.

T (°K)	$K_{sv} \times 10^4$	n	K_f (M^{-1})	ΔG (kJ M^{-1})	ΔH (kJ M^{-1})	ΔS (J M^{-1} K^{-1})
283	1.7	1.17	9.5×10^4	−27.35	–	–
298	1.8	1.36	1.38×10^5	−32.72	73.91	357.83
310	2.5	1.38	8.03×10^5	−37.02	–	–

[Cu(bpy)(L1)(H$_2$O)(C$_2$H$_5$OH)] (1.8 × 10^5 M^{-1}) [69], and 2,9(10),16(17),23(24)-tetrakis-[20,30,50,60-tetrafluoro-40-(2-dimethyl aminoethanethio)benzyloxy]phthalocyaninatozinc(II) tetraiodide (6.2 × 10^5 M^{-1}) [70] which bind to DNA via groove-binding mode.

3.2.4.1. *Determination of thermodynamic parameters.* The plot of log K_f versus $1/T$ (figure S8) allows calculation of the enthalpy (ΔH), entropy (ΔS) [equation (4)], and free energy (ΔG) change by the van't Hoff equation, equation (5), assuming that the enthalpy change (ΔH) is free of temperature over the range of applied temperatures.

$$\ln k = -\frac{\Delta H}{RT} + \frac{\Delta S}{R} \tag{4}$$

$$\Delta G = \Delta H - T\Delta S \tag{5}$$

Table 1 exhibits the thermodynamic values of the interaction of the complex with ct-DNA. According to the data of enthalpy changes (ΔH) and entropy changes (ΔS), the model of interaction between the complex and DNA can be concluded: (1) $\Delta H > 0$ and $\Delta S > 0$, hydrophobic forces; (2) $\Delta H < 0$ and $\Delta S < 0$, van der Waals interaction and hydrogen bonds; (3) $\Delta H < 0$ and $\Delta S > 0$, electrostatic interactions [71].

It can be seen that the negative value of ΔG revealed that the DNA interaction process is spontaneous; the positive ΔH and ΔS values indicated that hydrophobic forces play main roles in the binding of the complex to DNA.

3.2.4.2. *Iodide quenching studies.* Further support for groove binding of the complex to DNA is obtained through iodide quenching experiments. A highly negatively charged quencher is expected to be repelled by the negatively charged phosphate backbone of DNA; therefore, an intercalative bound compound should be protected from being quenched by anionic quencher. Free aqueous complexes or groove-binding ligands should be quenched readily by anionic quenchers [72]. The K_{sv} value of the bound ligand should be lower than that of the free ligand, if the small molecule is intercalated into the helix stack. In contrast, if a ligand binds to DNA in the groove, the value of K_{sv} of the bound ligand should be higher than that of the free ligand [73, 74]. Negatively charged I$^-$ was chosen for this purpose. The quenching constants (K_{sv}) are calculated from the Stern–Volmer equation. K_{sv} of the free copper complex by I$^-$ ion is 274.2 M^{-1} and in the presence of DNA, K_{sv} is 402.9 M^{-1} (shown in figure S9). The results displayed almost the same iodide quenching effect on the fluorescence of the complex before and after the interaction with DNA, which suggested that the complex binds to ct-DNA through groove-binding mode.

3.2.5. Molecular docking analysis. Computer docking techniques play an important role in drug design and elucidation of mechanism. The flexible docking programs AutoDock and molecular operating environment (MOE) help in predicting favorable DNA–ligand complex structures with reasonable accuracy and speed. These docking programs, when used prior to experimental screening, can be considered as powerful computational filters to reduce labor and cost for the development of effective medicinal compounds. When they are used after experimental screening, they can help in better understanding bioactivity mechanisms [75]. The docking is important in the study of various properties associated with DNA–ligand interactions, such as binding energy, geometry complementarily, electron

distribution, hydrogen bond, donor acceptor properties, hydrophobicity, and polarizability [76]. Adefovir dipivoxil is a prodrug which is converted to the active drug adefovir by pre-systemic metabolism in intra cell [1]. Similarly, *cis*-diammine dichloro platinum(II) complex is changed to *cis*-[diamminediaquaplatinum(II)] for attaching it to the DNA [77]. Therefore, molecular docking studies were carried out using a new structure of the complex (figure 6). In this structure, adefovir dipivoxil is replaced with adefovir, and Cl atom is replaced with H_2O. From the docking results with the optimal energy, it was found that the complex inserted into the groove of DNA fragments and hydrogen bonds play the main role in the binding of complex to DNA, while experimental results showed hydrophobic forces are main forces in the binding of the complex to DNA. The difference between experimental and computational methods can be due to conversion of adefovir dipivoxil to adefovir, and replacement of chloride to H_2O of the complex in cell environment. A hydrogen bond was observed between hydrogen of the complex with O_4-DC-23 with a bond length of 2.41 Å (figure 6). As shown in figure 7 from the docking calculation, the conformer with minimum binding energy is picked up from the 10 minimum energy conformers from the 100 runs. The run data for the conformers are listed in table 2. From the results of 10 sets, almost all the binding sites of the complex were located in the groove of double-helix DNAs. From the docking simulation, the observed free energy change of binding (ΔG) for the copper complex–DNA is calculated to be -5.74 kcal M^{-1}, which is slightly larger than the experimental free energy of binding (-5.45 kcal M^{-1}) obtained from the UV–vis data. This apparent mismatch in the free energy changes could be due to exclusion of the solvent and/or
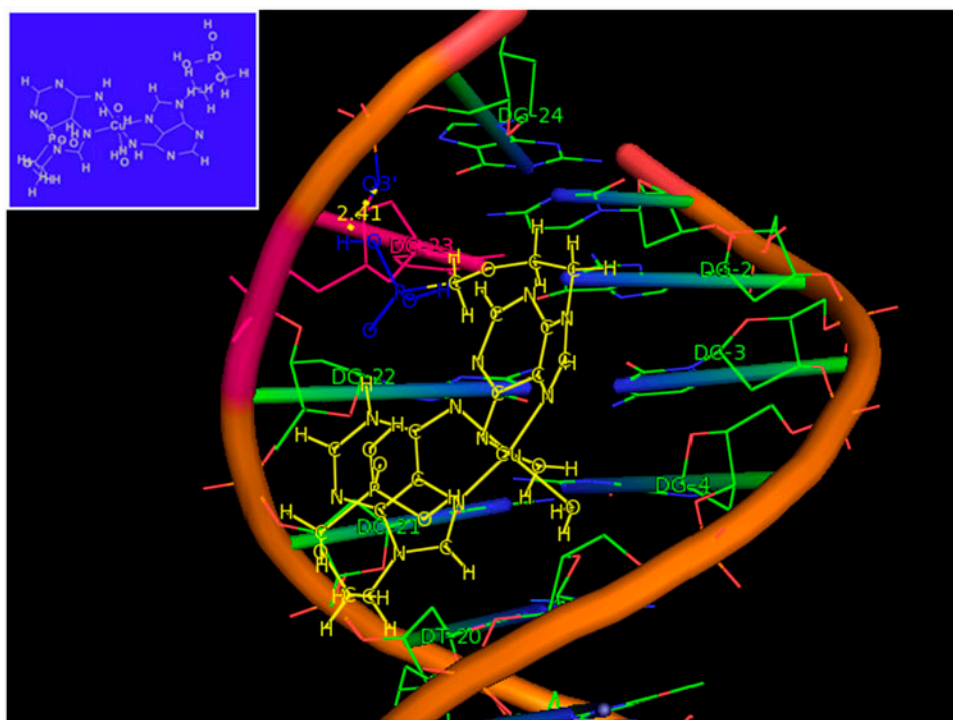

Figure 6.   Molecular modeling of the hydrogen-bonding interaction between the copper(II) complex and ct-DNA.
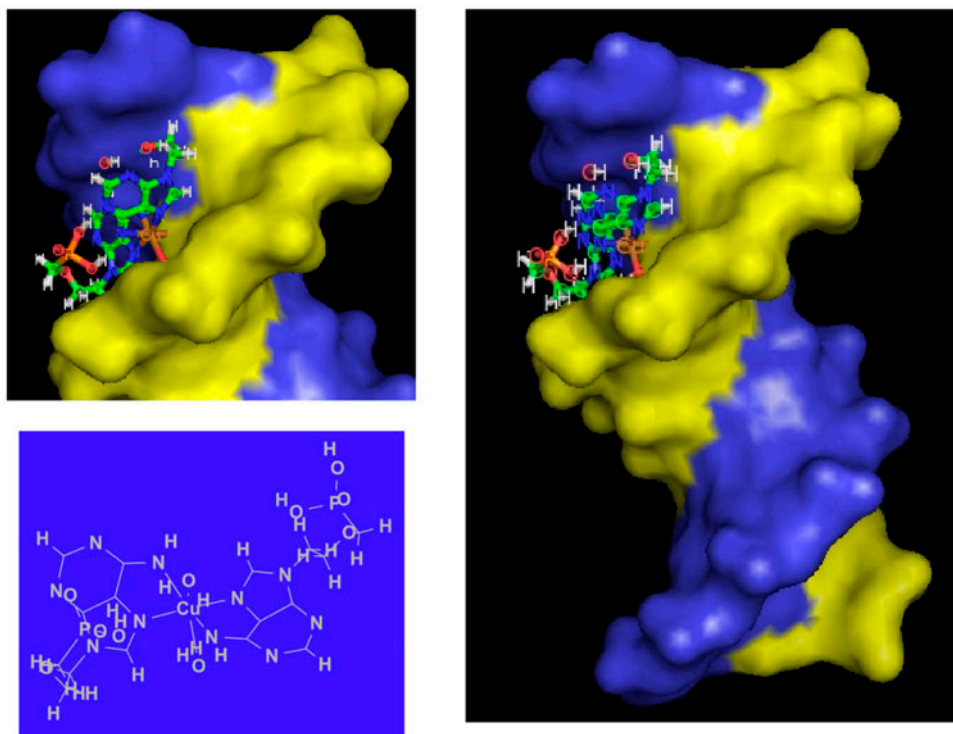
Figure 7.   Molecular docking perspective of the complex with the groove side of DNA.

Table 2.   Docking summary of DNA with the copper complex by the AutoDock program generating different ligand conformers using a Lamarkian GA.

Rank	Run	Binding energy (kcal M^{-1})	^aK_i (μM)	Cluster rmsd	Reference rmsd
1	**58**	**−5.74**	**62.05**	**0.00**	**19.57**
2	72	−5.46	99.24	0.00	25.36
3	13	−5.28	135.8	0.00	27.97
4	32	−4.97	227.68	0.00	25.79
5	68	−4.95	236.78	0.00	26.04
6	33	−4.85	279.77	0.00	20.28
7	88	−4.84	282.08	0.00	20.96
8	56	−4.83	406.82	0.00	28.88
9	92	−4.81	300.37	0.00	20.66
10	25	−4.62	412.95	0.00	28.61

^aK_i is the inhibition constant.

rigidity of some other receptor DNA in the molecular docking studies. Basic formula of binding constant and Gibbs free energy is:

$$\Delta G = -RT \ln K \tag{6}$$

The binding constant obtained by fluorescence data ($1.38 \times 10^5\ M^{-1}$) is slightly different to the binding constant calculated by docked copper complex–DNA model

$(1.7 \times 10^5 \text{ M}^{-1})$. Hence, it can be concluded that copper complex–DNA docked model is in approximate correlation with our experimental results [78].

4. Conclusion

We have synthesized a copper(II) complex, $[\text{Cu(adefovir)}_2\text{Cl}_2]$, which exhibits high binding affinity to ct-DNA. Different instrumental methods were used to find the interaction mechanism of the complex with ct-DNA. Upon addition of various concentrations of DNA in its UV spectrum, hyperchromism of the band at 261 nm was observed, suggesting the existence of a strong interaction between the complex and DNA. Groove-binding mode of interaction between DNA and $[\text{Cu(adefovir)}_2\text{Cl}_2]$ may result due to relatively small changes in DNA viscosity. The conformational change of DNA after binding with the complex was also confirmed using circular dichroism spectroscopy. Fluorescence study showed that the emission intensity of the copper complex was quenched by adding ct-DNA. This quenching can be attributed to photoelectron transfer from the guanine base of DNA to the excited levels of the complex. The free energy values for the compound at various temperatures are negative, showing the spontaneity of copper(II) complex–DNA binding. The results reveal that hydrophobic interactions play the most important contributions to the binding process with ct-DNA. Iodide quenching experiment displayed almost the same iodide quenching effect on the fluorescence of the complex before and after the interaction with DNA, which suggested that the complex binds to ct-DNA through groove binding. The docking results revealed that groove mechanism is for copper(II) complex binding with DNA. The results of spectroscopic techniques and molecular docking provide information about complex–DNA interaction, valuable for the rational design of new drugs that are more efficient as well as for understanding mechanism of these new drugs at the molecular level.

References

[1] X. Ming, D.R. Thakker. *Biochem. Pharmacol.*, **79**, 455 (2010).
[2] J. Fung, C.L. Lai, M.F. Yuen. *Drug Discovery Today Ther. Strategies*, **3**, 197 (2006).
[3] S.J. Hadziyannis, N.C. Tassopoulos, E.J. Heathcote, T.T. Chang, G. Kitis, M. Rizzetto, P. Marcellin, S.G. Lim, Z. Goodman, M.S. Wulfsohn. *New Engl. J. Med.*, **348**, 800 (2003).
[4] I. Kostova. *Curr. Med. Chem.*, **13**, 1085 (2006).
[5] I. Ott, R. Gust. *Archiv.Der. Pharmazie.*, **340**, 117 (2007).
[6] Z.A. Siddiqi, M. Khalid, S. Kumar, M. Shahid, S. Noor. *Eur. J. Med. Chem.*, **45**, 264 (2010).
[7] K.L. Haas, K.J. Franz. *Chem. Rev.*, **109**, 4921 (2009).
[8] S. Delaney, M. Pascaly, P.K. Bhattacharya, K. Han, J.K. Barton. *Inorg. Chem.*, **41**, 1966 (2002).
[9] F. Arjmand, S. Parveen, M. Afzal, L. Toupet, T. Ben Hadda. *Eur. J. Med. Chem.*, **49**, 141 (2012).
[10] J. Tan, B. Wang, L. Zhu. *Bioorg. Med. Chem.*, **17**, 614 (2009).
[11] S. Niroomand, M. Khorasani Motlagh, M. Noroozifar, A. Moodi. *J. Photochem. Photobiol. B*, 117, 132 (2012).
[12] M.J. Hannon. *Chem. Soc. Rev.*, **36**, 280 (2007).
[13] H.-L. Wu, K.T. Wang, B. Liu, F. Kou, F. Jia, J.K. Yuan, Y. Bai. *Inorg. Chim. Acta*, **384**, 302 (2012).
[14] B. Rosenberg, L. VanCamp, J.E. Trosko, V.H. Mansour. *Nature* (London), **222**, 385 (1969).
[15] F. Liang, C. Wu, H. Lin, T. Li, D. Gao, Z. Li, J. Wei, C. Zheng, M. Sun. *Bioorg. Med. Chem. Lett.*, **13**, 2469 (2003).
[16] G. Cerchiaro, K. Aquilano, G. Filomeni, G. Rotilio, M.R. Ciriolo, A.M.D.C. Ferreira. *J. Inorg. Biochem.*, **99**, 1433 (2005).
[17] C. Fernandes, G.L. Parrilha, J.A. Lessa, L.J. Santiago, M.M. Kanashiro, F.S. Boniolo, A.J. Bortoluzzi, N.V. Vugman, M.H. Herbst, A. Horn Jr. *Inorg. Chim. Acta*, **359**, 3167 (2006).

[18] X. Qiao, Z.Y. Ma, C.Z. Xie, F. Xue, Y.W. Zhang, J.Y. Xu, Z.Y. Qiang, J.S. Lou, G.J. Chen, S.P. Yan. *J. Inorg. Biochem.*, **105**, 728 (2011).
[19] B.L. Fei, W. Li, W.S. Xu, Y.G. Li, J.Y. Long, Q.B. Liu, K.Z. Shao, Z.M. Su, W.Y. Sun. *J. Photochem. Photobiol. B*, **125**, 32 (2013).
[20] P. Živec, F. Perdih, I. Turel, G. Giester, G. Psomas. *J. Inorg. Biochem.*, **117**, 35 (2012).
[21] R.R. Duan, L. Wang, W.Q. Huo, S. Chen, X.H. Zhou. *J. Coord. Chem.*, **67**, 2765 (2014).
[22] M. Iqbal, S. Ali, Zia-Ur-Rehman, N. Muhammad, M. Sohail, V. Pandarinathan. *J. Coord. Chem.*, **67**, 1 (2014).
[23] M.-L. Liu, M. Jiang, K. Zheng, Y.T. Li, Z.-Y. Wu, C.W. Yan. *J. Coord. Chem.*, **67**, 630 (2014).
[24] J. Lu, J.L. Li, Q. Sun, L. Jiang, B.-W. Wang, W. Gu, X. Liu, J.L. Tian, S.P. Yan. *J. Coord. Chem.*, **67**, 300 (2014).
[25] R.C. Santra, K. Sengupta, R. Dey, T. Shireen, P. Das, P.S. Guin, K. Mukhopadhyay, S. Das. *J. Coord. Chem.*, **67**, 265 (2014).
[26] S. Anbu, A. Killivalavan, E.C. Alegria, G. Mathan, M. Kandaswamy. *J. Coord. Chem.*, **66**, 3989 (2013).
[27] N. Raman, A. Sakthivel, R. Jeyamurugan. *J. Coord. Chem.*, **62**, 3969 (2009).
[28] N. Shahabadi, M. Falsafi. , *Spectrochim. Acta, Part A*, **125**, 154 (2014).
[29] G.M. Morris, R. Huey, W. Lindstrom, M.F. Sanner, R.K. Belew, D.S. Goodsell, A.J. Olson. *J. Comput. Chem.*, **30**, 2785 (2009).
[30] W.L. DeLano. The PyMOL molecular graphics system, (2002), Available online at: www.citeulike.org/group/340/article/240061.
[31] S.F. Tan, K.P. Ang, H.L. Jayachandran. *Transition Met. Chem.*, **9**, 390 (1984).
[32] B.C. Cornilsen, K. Nakamoto. *J. Inorg. Nucl. Chem.*, **36**, 2467 (1974).
[33] P. Drożdżewski, B. Pawlak. *Spectrochim. Acta, Part A*, **60**, 1527 (2004).
[34] F. Arjmand, A. Jamsheera, D. Mohapatra. *J. Photochem. Photobiol. B*, **121**, 75 (2013).
[35] M.A. Jakupec, M. Galanski, V.B. Arion, C.G. Hartinger, B.K. Keppler. *Dalton Trans.*, **2**, 183 (2007).
[36] X. Xu, D. Wang, X. Sun, S. Zeng, L. Li, D. Sun. *Thermochim. Acta*, **493**, 30 (2009).
[37] M. Sirajuddin, S. Ali, A. Badshah. *J. Photochem. Photobiol. B*, **124**, 1 (2013).
[38] A.E. Radi, A.E. El-Naggar, H.M. Nassef. *Electrochim. Acta*, **129**, 259 (2014).
[39] M. Arvin, G. Dehghan, M.A. Hosseinpourfeizi, A.A. Moosavi-Movahedi. *Spectrosc. Lett.*, **46**, 250 (2013).
[40] M.N. Nejat Dehkordi, P. Lincoln. *J. Fluoresc.*, **23**, 813 (2013).
[41] T. Zhao, S. Bi, Y. Wang, T. Wang, B. Pang, T. Gu. *Spectrochim. Acta, Part A*, **132**, 198 (2014).
[42] R. Vijayalakshmi, M. Kanthimathi, V. Subramanian, B.U. Nair. *BBA-Gen. Subjects*, **1475**, 157 (2000).
[43] R. Bera, B.K. Sahoo, K.S. Ghosh, S. Dasgupta. *Int. J. Biol. Macromol.*, **42**, 14 (2008).
[44] D.K. Jangir, S.K. Dey, S. Kundu, R. Mehrotra. *J. Photochem. Photobiol. B*, **114**, 38 (2012).
[45] F. Arjmand, S. Parveen, M. Afzal, M. Shahid. *J. Photochem. Photobiol. B*, **114**, 15 (2012).
[46] S. Tabassum, M. Zaki, F. Arjmand, I. Ahmad. *J. Photochem. Photobiol. B*, **114**, 108 (2012).
[47] G.S. Kurdekar, S. Mudigoudar Puttanagouda, N.V. Kulkarni, S. Budagumpi, V.K. Revankar. *Med. Chem. Res.*, **20**, 421 (2011).
[48] G. Barone, A. Terenzi, A. Lauria, A.M. Almerico, J.M. Leal, N. Busto, B. García. *Coord. Chem. Rev.*, **257**, 2848 (2013).
[49] M. Nandy, D.L. Hughes, G.M. Rosair, R.K.B. Singh, S. Mitra. *J. Coord. Chem.*, **67**, 3335 (2014).
[50] R.B. Devi, S.P. Devi, R.B. Singh, R.H. Singh, T. Swu, W.R. Devi, C.B. Singh. *J. Coord. Chem.*, **67**, 891 (2014).
[51] Z.C. Liu, B.D. Wang, Z.Y. Yang, Y. Li, D.D. Qin, T.R. Li. *Eur. J. Med. Chem.*, **44**, 4477 (2009).
[52] C.Y. Zhou, J. Zhao, Y.B. Wu, C.X. Yin, Y. Pin. *J. Inorg. Biochem.*, **101**, 10 (2007).
[53] S. Kashanian, A. Tahmasian Ghobadi, H. Roshanfekr, Z. Shariati. *Mol. Biol. Rep.*, **40**, 1173 (2013).
[54] Z. Zhang, W. Huang, J. Tang, E. Wang, S. Dong. *Biophys. Chem.*, **97**, 7 (2002).
[55] Y. Zhou, Y. Li. *Biophys. Chem.*, **107**, 273 (2004).
[56] C.S. Braun, G.S. Jas, S. Choosakoonkriang, G.S. Koe, J.G. Smith, C.R. Middaugh. *Biophys. J.*, **84**, 1114 (2003).
[57] N.J. Zuidam, Y. Barenholz, A. Minsky. *FEBS Lett.*, **457**, 419 (1999).
[58] C. Zimmer, U. Wähnert. *Prog. Biophys. Mol. Biol.*, **47**, 31 (1986).
[59] L.F. Tan, H. Chao, H. Li, Y.J. Liu, B. Sun, W. Wei, L.N. Ji. *J. Inorg. Biochem.*, **99**, 513 (2005).
[60] P. Xi, Z. Xu, X. Liu, F. Cheng, Z. Zeng. *Spectrochim. Acta, Part A*, **71**, 523 (2008).
[61] A.S. El Tabl, F.A. El Saied, W. Plass, A.N. Al-Hakimi. , *Spectrochim. Acta, Part A*, **71**, 90 (2008).
[62] I. Berlman. *Handbook of Florescence Spectra of Aromatic Molecules*, Elsevier, Burlington (2012).
[63] B. Valeur, M.N. Berberan Santos, *Mol. Fluoresc. Principles Applications*, John Wiley & Sons, Weinheim (2012).
[64] H. Chen, S.S. Ahsan, M.E.B. Santiago-Berrios, H.D. Abruña, W.W. Webb. *J. Am. Chem. Soc.*, **132**, 7244 (2010).
[65] Y.J. Hu, H.-G. Yu, J.X. Dong, X. Yang, Y. Liu. *Spectrochim. Acta, Part A*, **65**, 988 (2006).
[66] Y.J. Hu, Y. Liu, X.H. Xiao. *Biomacromolecules*, **10**, 517 (2009).

[67] F.F. Tian, F.L. Jiang, X.L. Han, C. Xiang, Y.S. Ge, J.H. Li, Y. Zhang, R. Li, X.L. Ding, Y. Liu. *J. Phys. Chem. B*, **114**, 14842 (2010).
[68] B.K. Sahoo, K.S. Ghosh, S. Dasgupta. *Biopolymers*, **91**, 108 (2009).
[69] K. Rupesh, S. Deepalatha, M. Krishnaveni, R. Venkatesan, S. Jayachandran. *Eur. J. Med. Chem.*, **41**, 1494 (2006).
[70] M. Özçeşmeci, Ö.B. Ecevit, S. Sürgün, E. Hamuryudan. *Dyes Pigm.*, **96**, 52 (2013).
[71] B. Valeur, J.C. Brochon, *New Trends in Fluorescence Spectroscopy: Applications to Chemical and Life Sciences: With 187 Figures and 39 Tables*, Springer, Berlin (2001).
[72] J.R. Lakowicz, B.R. Masters. *J. Biomed. Opt.*, **13**, 9901 (2008).
[73] A. Bozzi, T. Yuranova, I. Guasaquillo, D. Laub, J. Kiwi. *J. Photochem. Photobiol. A*, **174**, 156 (2005).
[74] X. Ling, W. Zhong, Q. Huang, K. Ni. *J. Photochem. Photobiol. B*, **93**, 172 (2008).
[75] F. Perveen, R. Qureshi, A. Shah, S. Ahmed, F.L. Ansari, S. Kalsoom, S. Mehboob. *Int. Res. J. Pharm.*, **1**, 1 (2011).
[76] A.-N. Alaghaz, B.A. El Sayed, A.A. El Henawy, R.A. Ammar. *J. Mol. Struct.*, **1035**, 83 (2013).
[77] F. Bernges, G. Dorner, E. Holler. *Eur. J. Biochem.*, **191**, 743 (1990).
[78] A. Abderrezak, P. Bourassa, J.S. Mandeville, R. Sedaghat-Herati, H.A. Tajmir Riahi. *PLoS ONE*, **7**, e33102 (2012).